Radio Science, Volume 35, Number 2, Pages 385–394, March–April 2000

Modeling ELF radio atmospheric propagation and extracting lightning currents from ELF observations

Steven A. Cummer[1]
Laboratory for Extraterrestrial Physics, NASA Goddard Space Flight Center, Greenbelt Maryland

Umran S. Inan
Space, Telecommunications and Radioscience Laboratory, Stanford University, Stanford, California

Abstract. Observations of extremely low frequency (ELF) radio atmospherics (sferics), the transient electromagnetic fields radiated by lightning discharges, are used to determine the current moment waveforms of vertical lightning discharges. In order to extract this information the propagation of radio atmospherics from source to receiver must be modeled accurately, especially in view of the important role played by the D and E regions of the ionosphere at these long (>200 km) wavelengths. We model broadband ELF sferic waveforms by adapting a single-frequency ELF propagation code to calculate an ELF propagation impulse response under the assumption of horizontal ionospheric homogeneity, with which we extract the source lightning current waveform from an observed ELF sferic waveform using a deconvolution method based on linear regularization. Tests on modeled sferics indicate that the method is accurate and relatively insensitive to noise, and we demonstrate the application of the technique with a sprite-associated sferic. Since ELF sferics can often be observed many thousands of kilometers from the source discharge, the technique developed here represents a powerful new method of remotely sensing lightning current waveforms.

1. Introduction

Radio atmospherics (or sferics, for short) are the electromagnetic signals launched by individual lightning discharges. Lightning radiates electromagnetic energy over an extremely wide bandwidth, from a few hertz [*Burke and Jones*, 1992] to many tens of megahertz [*Weidman and Krider*, 1986]. However, by virtue of the timescales of the return stroke current most of the energy is radiated in the very low frequency (VLF, 3–30 kHz) and extremely low frequency (ELF, 3–3000 Hz) bands. ELF and VLF energy originating in a lightning discharge is reflected by the lower ionosphere and the ground and thus propagates in a guided fashion between these two boundaries, which form what is known as the Earth-ionosphere waveguide. This guided propagation occurs with low attenuation rates (a few decibels per 1000 km [*Taylor and Sao*, 1970]), allowing ELF-VLF sferics to be observed literally around the world from their source lightning discharge.

Since ELF-VLF sferics are launched by the lightning current and can be observed at long distances from the discharge, their measurement can potentially provide a powerful technique for remotely sensing the source lightning current waveform. In this work, we develop a technique to determine the lightning discharge current moment (i.e., current magnitude times channel length) using ELF sferics measured at an arbitrary but known distance from the source lightning. We assume that the propagation

[1]Now at Department of Electrical and Computer Engineering, Duke University, Durham, North Carolina.

Paper number 1999RS002184.
0048-6604/00/1999RS002184$11.00

of this energy is linear, and therefore we ignore any ionospheric modification by the radiated lightning energy. Although intense lightning discharges produce both heating and ionization at ionospheric altitudes [*Taranenko et al.*, 1993], such disturbances are generally localized, and their effects on ELF sferics at long distances are expected to be small. This linearity implies that the sferic waveform is given by the convolution of the source current moment and the overall system impulse response, defined as the fields observed remotely from an impulsive vertical lightning discharge, which includes the effects of signal propagation and reception. Thus the extraction of the current moment amounts to a deconvolution of the observed ELF sferic and an appropriate propagation impulse response, which we implement with a technique known as linear regularization. We model the propagation impulse response by adapting a general, single-frequency ELF-VLF propagation code (Long Wave Propagation Capability, or LWPC) [*Pappert and Moler*, 1974; *Pappert and Ferguson*, 1986] to model broadband ELF sferic waveforms.

To simplify the extraction of the source current moment, we only consider the propagation of the quasi-transverse electromagnetic (QTEM) mode in a horizontally homogeneous Earth-ionosphere waveguide (although inhomogeneities can be accounted for if required). Our assumption of homogeneity is valid at midlatitudes at night when the ionosphere is relatively stable, but it breaks down in regions of known inhomogeneity such as the day-night terminator. Since the QTEM mode is inefficiently excited by a horizontal current source, our method is effectively limited to measuring vertical currents. Although the sferic waveforms received on the ground are composed of a superposition of this QTEM mode and other waveguide modes, the desired QTEM mode can be extracted by low-pass filtering the sferics at ~1.5 kHz, as the quasi-transverse electric (QTE) and quasi-transverse magnetic (QTM) modes typically have a sharp cutoff near this frequency and thus do not contain significant energy below it [e.g., *Cummer et al.*, 1998a]. This filtering necessarily limits the bandwidth of the extracted current moment and therefore precludes the extraction of current waveform characteristics with frequencies above 1.5 kHz. It should be noted that while this filtering does increase the risetime and fall time of the discharge current and reduces the peak current amplitude, it does not significantly reduce the measurability of the total charge moment change in the discharge (i.e., the time integral of the current moment), which is an important quantity in some applications. The bandwidth of the measurement could be increased by including the information at frequencies above ~1.5 kHz; however, the propagation of VLF energy in the QTE and QTM modes is highly dispersive and depends strongly on the ionosphere [*Cummer et al.*, 1998a], making it more difficult to analyze than the signal in the QTEM mode. These highly dispersed QTE modes are responsible for the waveforms known as tweeks [*Sukhorukov*, 1996]. We should also mention that we use the term ELF throughout this work to denote signal energy at frequencies where only the QTEM mode propagates (below ~1.5 kHz).

Among the techniques that have been used to measure lightning return stroke current waveforms and charge transfer are direct strike of instruments [*Hubert et al.*, 1984], electric field mill arrays [*Krehbiel et al.*, 1979], and nearby observations of HF radiation [*Cooray and Gomes*, 1998]. A disadvantage of these techniques is that they are restricted to measurements made at distances of at most a few tens of kilometers from the lightning discharge. The sferic-based method which we describe in this work can be applied to any observable sferic with a known source location and thus does not have a localization limitation. The sferic-based technique outlined here has been particularly useful in the measurement of charge transfer in lightning discharges which are associated with sprites [e.g., *Cummer et al.*, 1998b], the transient mesospheric optical emissions which occur in response to some strong lightning discharges.

ELF sferics, also referred to as "slow tails," have been studied experimentally for many years [*Hepburn*, 1957; *Taylor and Sao*, 1970; *Hughes*, 1971; *Burke and Jones*, 1992; *Reising et al.*, 1996]. *Burke and Jones* [1996] described a method to extract a two-parameter lightning current moment from measured ELF sferics in a narrow frequency range (5–50 Hz), while our technique extracts an arbitrary lightning current moment waveform over a wider bandwidth (~10–1500 Hz). A number of simplified, analytical models of single-frequency and broadband ELF propagation have been formulated [*Wait*, 1960; *Jones*, 1970; *Greifinger and Greifinger*, 1978, 1979, 1986; *Sukhorukov*, 1992], most of which require an exponentially varying ionospheric conductivity. An ELF propagation impulse response calculated with any of these other methods can be used with the deconvolution method described in section 3.1 to ex-

tract a lightning current moment waveform. However, the LWPC-based propagation model that we use is perhaps the most general, allowing for a completely arbitrary and more realistic ionosphere.

2. ELF Sferic Modeling

As mentioned in section 1, we wish to calculate the ELF electric and magnetic fields radiated by an arbitrary vertical lightning current waveform. Although the detailed dynamics of a lightning return stroke are complicated [*Thottappillil et al.*, 1997], we can treat the discharge channel as an electrically short antenna having a time-varying current that is constant along the channel length. This approximation is valid because we restrict our analysis to frequencies $f < 1.5$ kHz where the wavelength ($\lambda > 200$ km) is much longer than the typical channel length ($l < 10$ km) and because the radiated fields are nearly independent of source altitude for propagation in the QTEM mode [*Cummer et al.*, 1998b] for altitudes below the ionosphere. Thus the radiation source is the current moment waveform $m_i(t) = li(t)$, where l is the lightning current length and $i(t)$ is the current waveform. Because this propagation problem is linear and time invariant, the fields are related to an arbitrary current waveform by a simple convolution operation [*Bracewell*, 1986, p. 24], and it is sufficient to consider the fields produced by an impulsive current, which we refer to as the propagation impulse response. This impulse response is equivalently the Green's function for fields from an impulsive source for a specific and known source-receiver distance.

Propagation in a horizontally homogeneous waveguide like that considered here can be modeled efficiently by Fourier transform methods, from which a time domain waveform can be computed as the inverse Fourier transform of the frequency domain solution. This is the solution method we use in this work. When inhomogeneities are expected to play a major role, direct time domain (finite difference or finite element) methods become more useful.

The shape of an ELF waveform is strongly controlled by the bandwidth of the receiver with which it is observed. Consequently, we must apply the effective receiver filters to any modeled ELF waveform or impulse response so that it is directly comparable to the observed ELF sferics. Such filtering ensures that the modeled ELF impulse response is the impulse response of the entire system, including propagation and receiver effects. It is also possible to digitally filter the measured sferics after observation to impose a different frequency response, provided that the receiver response is flat at the frequencies where such postfiltering is applied. The frequency response of the receiver used in this work is flat to below 1 Hz [*Fraser-Smith and Helliwell*, 1985], and we impose a single-pole, 30 Hz high-pass filter to the observed and modeled sferics and spectra presented here. As discussed in section 3.2, this low frequency response can play a role in the detectability of slowly varying currents, so that we must keep the lower cutoff as low as possible, but not so low that the so-called Schumann resonances [*Nickolaenko*, 1997] contribute significantly to the observed signal. We also must apply a low-pass filter to the observed sferics in order to remove the QTM and QTE portions of the signal (which, as discussed in section 1, are only significant for $f > 1.5$ kHz), and we must apply the same filter to the modeled ELF impulse response for accurate comparison of modeled and measured sferics. This filter, which we implement as a thirtieth-order digital finite impulse response (FIR) filter with a -3 dB cutoff frequency of 1 kHz, is applied to all the waveforms and spectra in this work.

2.1. Frequency Domain Modeling

As the basis of our broadband ELF sferic propagation model, we use the single-frequency LWPC ELF-VLF propagation model [*Pappert and Ferguson, 1986*]. This general model allows for arbitrary orientation of the ambient magnetic field, arbitrary homogeneous ground permittivity and conductivity, and arbitrary altitude profiles of ionospheric electron and ion density. For ELF propagation, LWPC solves the time harmonic (i.e., single frequency) propagation problem using mode theory [*Budden*, 1961], in which the fields at a distance from the source are produced by the QTEM waveguide mode. This mode, which is analogous to the TEM mode of a perfectly conducting parallel plate waveguide, is composed primarily of a horizontal magnetic field perpendicular to the propagation direction and a vertical electric field. For example, the transverse horizontal magnetic field B_y at a distance x along the ground from a vertical electric dipole source as a function of frequency is

$$B_y(\omega, x) = -\mu_0 k^{1/2} M_e(\omega) \left[R_E \sin\left(\frac{x}{R_E}\right) \right]^{-1/2} \cdot \left(\frac{\pi}{2}\right)^{-1/2} e^{i\pi/4} \Lambda_t(\omega) \Lambda_r(\omega) e^{-ikx \sin\theta(\omega)}, \quad (1)$$

where wavenumber k is given by $k = 2\pi/\omega$, $M_e(\omega)$ is the vertical electric dipole moment of the source (and is related to the source current moment by $M_e(\omega) = -iM_i(\omega)/\omega$, where M_i is the source current moment amplitude) and the term $[R_E \sin(x/R_E)]^{-1/2}$ accounts for the spreading of the fields over a spherical Earth of radius R_E (note that this term is equivalent to $x^{-1/2}$ over short distances). The index of refraction of the QTEM mode is given by the sine of the corresponding eigenangle θ. The excitation and receiver factors Λ_t and Λ_r quantify the coupling between the transmitting and receiving antennas and the fields of the waveguide mode. These terms also contain the altitude dependence of the fields, but since all sources and receivers are assumed to be at ground altitude, their altitude dependence is omitted. The terms θ, Λ_t, and Λ_r are functions of frequency and depend on the specified ionospheric electron density and collision frequency profiles. They are all calculated numerically in the propagation code. The reader is referred to *Pappert and Ferguson* [1986, and references therein] for further details concerning this model.

To calculate the fields from a broadband source, one simply needs to calculate $B_y(\omega)$ over the range of frequencies significant to the problem at hand (in our case, ~10–2000 Hz). Figure 1 shows representative nighttime and daytime electron density (N_e) altitude profiles, and Figure 2 shows the ELF sferic amplitude spectra calculated with this model for these two profiles. The profiles are representative midlatitude local midnight and midday profiles calculated with the 1995 International Reference Ionosphere [*Rawer et al.*, 1978]. The positive ion density, which plays a significant role in nighttime ELF propagation, is taken to be equal to the electron density except where $N_e < 100$ cm^{-3}, at which altitudes the positive and negative ion densities are both set to 100 cm^{-3}. The spectra in Figure 2 are the amplitude of the transverse horizontal magnetic field B_y as a function of frequency observed at $x = 1000$, 2000, and 3000 km from the source discharge. The source current for each is an impulse with a total charge moment change of 10 C km. The peaks in the nighttime spectral amplitudes are a consequence of the realistic nighttime ionosphere; if the E region valley between 100 and 150 km is filled (as it is for the daytime profile), these peaks disappear. Similar resonance effects have been seen in theoretical studies of ELF propagation in the presence of narrow sporadic E layers [*Barr*, 1977], indicating that electron densities at these fairly high altitudes can strongly influence ELF propagation. The daytime ionosphere is much simpler, and under these conditions, approximate analytic formulations of ELF propagation with exponentially varying ionospheric conductivity [e.g., *Greifinger and Greifinger*, 1978; *Sukhorukov*, 1992] provide results similar to those of the full wave LWPC model.

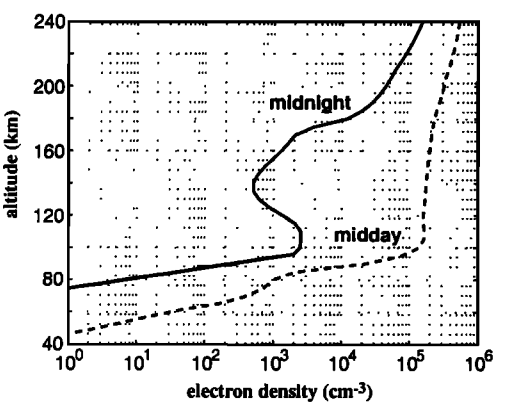

Figure 1. Representative daytime and nighttime ionospheric electron density profiles from the 1995 International Reference Ionosphere model.

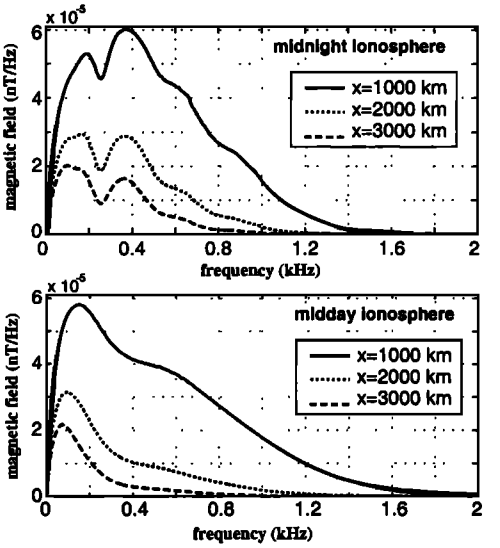

Figure 2. Calculated ELF sferic spectra for propagation distances of 1000, 2000, and 3000 km under nighttime and daytime ionospheres. The source is an impulsive discharge with a charge moment change of 10 C·km

2.2. Calculating a Time Domain Waveform

The complex sferic spectrum which results from our frequency domain calculation (e.g., Figure 2) is the Fourier transform of the sferic waveform and thus can be converted to a time domain waveform with an inverse Fourier transform operation. However, since we have only a sampled version of the continuous sferic spectrum $F(\omega)$ for positive ω, we must approximate the inverse Fourier transform, and we can do so using a method based on the fast Fourier transform (FFT).

The continuous time domain waveform $f(t)$ is defined by the inverse Fourier transform, namely, $f(t) = \frac{1}{2\pi}\int_{-\infty}^{+\infty} F(\omega)\exp(i\omega t)d\omega$. Taking advantage of the fact that $f(t)$ must be causal and therefore $F(\omega)$ must have Hermitian symmetry [*Bracewell*, 1986, p. 16], we can approximate $f(t)$ by

$$F(t) \approx \mathrm{Re}\left[\frac{\Delta\omega}{\pi}\sum_{m=0}^{N-1} F(m\Delta\omega)\exp(im\Delta\omega t)\right], \quad (2)$$

where $\Delta\omega$ is the difference between frequency samples and N is the number of samples of $F(\omega)$ calculated through (1). Using the standard definition of the inverse FFT of $\mathrm{IFFT}(X) = x_n = \frac{1}{N}\sum_{m=0}^{N-1} X_m \exp(i2\pi mn/N)$, a sampled version of $f(t)$ can be written as

$$f(n\Delta t) \approx \frac{N\Delta\omega}{\pi}\,\mathrm{Re}\{\mathrm{IFFT}[F(m\Delta\omega)]\}, \quad (3)$$

where $\Delta t = \frac{2\pi}{N\Delta\omega}$. In practice, $\Delta\omega = 2\pi \cdot 5$ Hz is sufficiently small to capture the finer spectral variations, and since the signal is essentially zero for frequencies greater than 2 kHz, a waveform sampling period of $\Delta t = 10^{-4}$ s meets the Nyquist criterion and results in a relatively smooth waveform. Together, these values require $N = 2000$, which corresponds to a maximum calculated frequency of $\omega_{\max} = 2\pi \cdot 10$ kHz. Since, as we mentioned, $|F(\omega)| \approx 0$ for $f > 2$ kHz, $F(\omega)$ need only be calculated up to 2 kHz and can be subsequently zero-padded to meet this requirement. The 1 kHz low-pass filtering described in section 2, which is applied to eliminate any contributions to the signal from the QTM and QTE modes, ensures that $|F(\omega)| \approx 0$ for $f > 2$ kHz.

Figure 3 shows the calculated B_y waveforms for the three propagation distances and two ionospheres for which the spectra were shown in Figure 2. These waveforms were filtered with the previously described high- and low-pass filters.

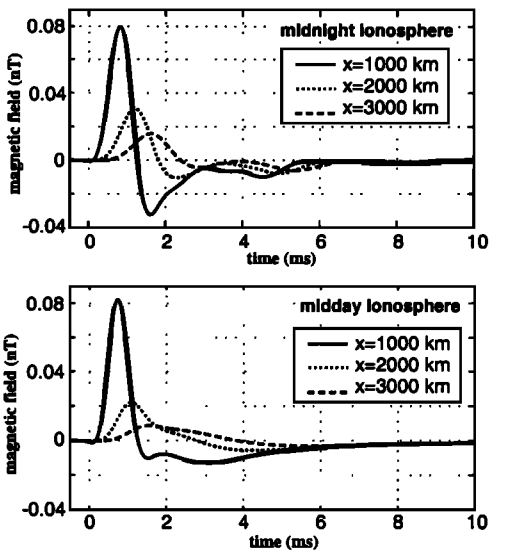

Figure 3. Calculated ELF B_y waveforms for propagation distances of 1000, 2000, and 3000 km under nighttime and daytime ionospheres. The source is an impulsive discharge with a charge moment change of 10 C km

3. Extracting the Source Current

The linearity and time invariance (on the millisecond timescales of individual sferics) of the propagation problem means that the relationship between the sferic waveform, current moment waveform, and propagation impulse response is a simple convolution, so that

$$f(t) = \int_{-\infty}^{\infty} m_i(\tau)\, h(t-\tau)\, d\tau, \quad (4)$$

where $h(t)$ is the propagation impulse response, $m_i(t)$ is the source current moment, and $f(t)$ is the observed electric or magnetic field waveform. Suppose that we have observed a given sferic for which we know the propagation distance from discharge to receiver and can therefore model the ELF propagation impulse response $h(t)$. We can extract the source current moment by solving the inverse convolution (or deconvolution) problem. However, unlike convolution, deconvolution is not a straightforward operation because of the nonunique nature of the problem. In our case, convolution is very similar to a low-pass filtering operation and therefore removes information contained in the higher frequencies of $m_i(t)$. This lost information cannot be recovered, and therefore

there are many waveforms $m_i(t)$ that satisfy the forward convolution problem almost equally well.

There are a number of deconvolution techniques which handle this nonuniqueness as well as other requirements on our solution (such as positivity of $m_i(t)$), many of which come from the related two-dimensional problem of image reconstruction [*Bracewell*, 1995, p. 453]. One technique which we have used successfully in the past is CLEAN [*Segalovitz and Frieden*, 1978], but linear regularization has proved to be a better method for our needs.

3.1. Linear Regularization

Since *Press et al.* [1992, p. 799] give a good discussion of the general technique of linear regularization, we only briefly summarize the method here. The convolution in (4) can be approximated in discrete form by the matrix equation $\mathbf{f} = \mathbf{A}\mathbf{i}$, where $\mathbf{f}$ and $\mathbf{i}$ are column vectors of length m and n containing the samples of $f(t)$ and $m_i(t)$, respectively, and where $\mathbf{A}$ is an $m \times n$ matrix with columns containing samples of $h(t)$ ($\mathbf{h}$) shifted by one sample relative to each other. In our problem, $\mathbf{A}$ and $\mathbf{f}$ are known, and we wish to find $\mathbf{i}$. Since, in general, $m \neq n$, an appropriate $\mathbf{i}$ is a least squares solution which minimizes the functional $|\mathbf{A}\mathbf{i} - \mathbf{f}|^2$. However, it is essentially impossible to find a reasonable $\mathbf{i}$ directly by this method because of the ill-conditioned nature of this problem.

The central idea of linear regularization is to add an additional term to the least squares functional which enforces smoothness on the solution $\mathbf{i}$, which often leads to a well-conditioned problem. There are a number of slightly different techniques for doing this, and the one we have found to work well in our application is to add to the functional we wish to minimize a factor proportional to the energy of the first difference of the signal energy, namely,

$$|\mathbf{A}\mathbf{i} - \mathbf{f}|^2 + \lambda \frac{\|\mathbf{h}\|_2}{\|\mathbf{f}\|_2} |\mathbf{B}\mathbf{i}|^2, \tag{5}$$

where $\mathbf{B}$ is as defined by *Press et al.* [1992, p. 800, equation 18.5.1]. This specific smoothing functional serves to minimize the difference of the solution i from a constant. The $\|\mathbf{h}\|_2/\|\mathbf{f}\|_2$ term is a normalizing factor so that $\lambda = 1$ is a reasonable choice. The left-hand term of (5) enforces correctness (in the context of deconvolution) on the solution $\mathbf{i}$, while the right-hand term enforces smoothness by minimizing the deviation of $\mathbf{i}$ from a constant. The factor λ controls the trade-off between these two competing solution requirements.

The normal equations for minimizing this functional are given by

$$\left(\mathbf{A}^T\mathbf{A} + \lambda \frac{\|\mathbf{h}\|_2}{\|\mathbf{f}\|_2} \mathbf{B}^T\mathbf{B}\right) \mathbf{i} = \mathbf{A}^T\mathbf{f}. \tag{6}$$

Because the matrix $\left(\mathbf{A}^T\mathbf{A} + \lambda \frac{\|\mathbf{h}\|_2}{\|\mathbf{f}\|_2} \mathbf{B}^T\mathbf{B}\right)$ is well conditioned, (6) can be solved for $\mathbf{i}$ using the usual techniques for the solution of a linear set of equations, such as LU decomposition or iterative methods like the conjugate gradient method.

To be physically reasonable, our solution $\mathbf{i}$ must be causal; that is, the current must be zero before the sferic starts, and it also must be strictly positive (because the vertical current in a single lightning discharge does not change direction). The direct solution of (6) does not guarantee either of these; thus they must be enforced through another technique. One technique that accomplishes this is the method of projections onto convex sets (POCS) [*Press et al.*, 1992, p. 804], which we implement in our solution to enforce causality and nonnegativity in our solution.

We do not believe that our use of linear regularization introduces any systematic biases in the extraction of a source current. Our choice of the deviation from a constant for a regularizing functional preferentially selects constant, positive currents and thus could lead to an overestimation of the total charge moment change. However, comparisons with a minimum total energy regularizing functional (which minimizes the total charge moment change and thus could lead to a systematic underestimation of the total charge moment change) show very little difference between these two techniques.

3.2. Testing the Deconvolution Method

We now test the linear regularization technique described in section 3.1 on a model ELF propagation problem. We assume a 2000 km propagation distance under the nighttime ionosphere shown in Figure 1. Figure 3 shows the calculated propagation impulse response for this scenario. Figure 4a shows the modeled sferic waveform calculated via convolution of this impulse response with the model source current moment waveform shown in Figure 4b. Filtered Gaussian noise with an amplitude of ~0.01 nT and frequency content up to ~500 Hz (this is an ap-

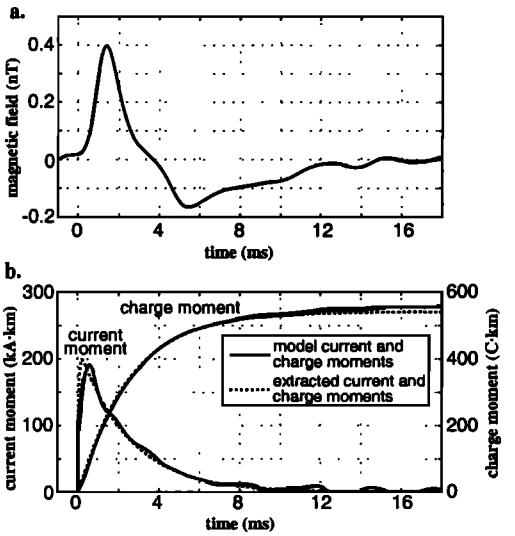

Figure 4. A test of the deconvolution method. (a) The noisy modeled sferic and the extracted sferic formed by the convolution of the propagation impulse response in Figure 3 and the extracted current moment. (b) The actual and extracted current moment waveforms.

proximation of the ELF noise which remains after removing most of the power line noise) has been added to this modeled sferic to simulate an actual observation. This sferic has also been filtered with the low-pass filter previously described in section 2.

Figure 4b compares the actual current moment waveform and charge moment change with those extracted from the noisy sferic (with λ=0.1). This deconvolution technique is clearly robust in the presence of noise, as the extracted current waveform is quite close to the model source current. The fact that the extracted current is unable to match the fast rise of the actual current is due to the limited bandwidth of the sferic used to extract the current. When combined with causality enforcement, the bandwidth limitation leads to a small reduction in the extracted charge transfer. Also, there is a significant deviation in the extracted charge moment change from the actual charge moment change beginning ~10 ms after the discharge onset, which is due to the fact that the additive noise begins to dominate the signal at this time. This deviation highlights the general fact that this method (and any method, for that matter) has problems when the signal to noise ratio (SNR) is low. Because the sferic amplitude generally decays with time, this fact prohibits extracting accurate source currents beyond some time after sferic onset. This time is generally later for larger sferic amplitudes (therefore with better SNR) and for lower low frequency receiver cutoff frequencies (thereby providing more signal at the lowest frequencies).

4. Application to an Observed Sferic

We now demonstrate the application of this technique to an actual observed sferic. The unfiltered magnetic field waveform shown in Figure 5a was received at Stanford University on July 24, 1996, at 0531:30.109 UT. The quasi-periodic power line noise has been removed by subtracting a noise-only signal period from the sferic plus noise period of interest. The propagation distance was 1888 km as measured by the National Lightning Detection Network (NLDN) [*Cummins et al.*, 1998]. This particular discharge was associated with a large sprite recorded on video at the Yucca Ridge Field Station [*Lyons*,

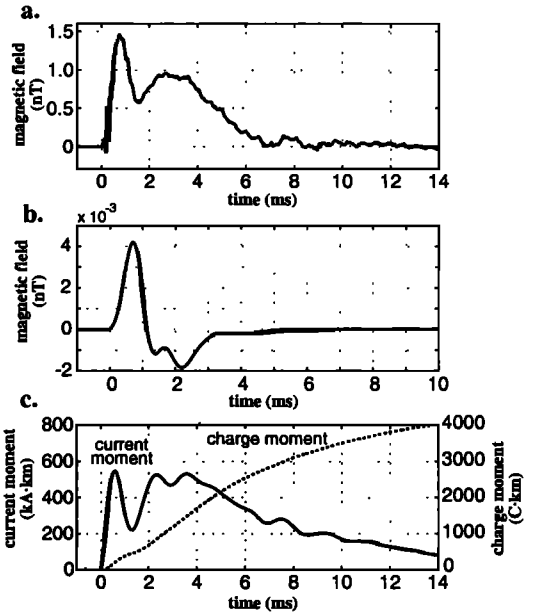

Figure 5. An application of the overall current measurement technique. (a) An observed ELF sferic. (b) The modeled ELF propagation impulse response for a source-receiver distance of 1888 km. (c) The charge moment waveform and cumulative charge moment change extracted from the observed sferic.

1996]. Since this discharge occurred at night, we employ in our model a nighttime ionosphere similar to that shown in Figure 1, and our ELF sferic model produces the magnetic field impulse response shown in Figure 5b. Applying the linear regularization deconvolution technique with $\lambda = 0.1$ yields the source current moment waveform and charge moment change shown in Figure 5c. The precision of this measurement can be demonstrated by a comparison between the filtered observed sferic and the reconstructed sferic formed by the convolution of this source current and the modeled impulse response. Graphically, these two waveforms are nearly indistinguishable, and their agreement can be quantified by the norm of the difference of the observed sferic (s_o) and reconstructed sferic (s_r) divided by the norm of s_o. Calculating this for the first 20 ms of the sferics, we find that $\|s_r - s_o\|_2 / \|s_o\|_2 = 0.020$, indicating that the mean deviation between the two waveforms is ~2%.

We should reemphasize that this deduced current moment is, in effect, a low-pass filtered version of the actual source current because of the bandwidth limitation of the observed sferics used in the calculation. Thus the measured current risetimes and peak currents are likely slower and lower, respectively, than in the actual lightning current. However, the cumulative charge moment change is measured accurately because of the smoothing nature of the integration required to calculate it. This feature makes the technique described here very powerful for remotely measuring charge moment changes.

There are a number of potential error sources in making a measurement of source current from observed ELF sferics. This technique requires an absolute calibration of the ELF receiver, and the Stanford receiver used in this work has a calibration error of ~5%. Because we do not know the state of the ionosphere all along the propagation path, there is always some difference between the modeled impulse response we use and the actual propagation impulse response. We have assessed this error by applying the technique to a single sferic with a range of reasonable ionospheric profiles, which indicates a ~5% variability in the extracted charge moment magnitudes. As discussed in section 3.2, the error most difficult to quantify is that associated with the signal noise. This error can be significant, especially at later times when the current varies slowly, and one must be careful not to place too much significance on currents extracted at times when the SNR is low.

5. Summary and Conclusions

We have presented a technique by which lightning currents can be measured remotely from ELF observations of the radiated electric or magnetic field waveforms. This new technique has two components. The first is an accurate model of the propagation of the ELF energy from source to receiver which is used to invert the measurements. We developed such a broadband ELF propagation model based on the general, single-frequency LWPC ELF-VLF propagation model, in which we assume a horizontally homogeneous ionosphere. The second component is the deconvolution technique by which the source current moment can be extracted from the observed ELF sferic and the modeled ELF impulse response. We found linear regularization to be a useful deconvolution method for this problem, and we showed that the overall technique is robust in the presence of noise and demonstrated the application of this technique to extract the source current moment from observed sferics.

Because sferics propagate in the low-loss waveguide formed by the Earth and ionosphere and can therefore be observed very long distances from the source lightning (as far as around the world in the case of high-amplitude sferics), the technique described here represents a powerful method by which lightning currents can be measured over a large geographic area with a single receiver. Because the sferic frequencies used in this technique are limited to less than ~1.5 kHz, the extracted source currents can be considered low-pass-filtered versions of the actual lightning current. While this fact effectively limits the measurable risetime of the source current and tends to reduce the measured peak currents, it does not limit the measurability of the total charge transfer in the discharge. For this reason this ELF technique has proved very useful in measuring lightning currents and charge transfers on millisecond timescales, such as those associated with sprites [*Cummer et al.*, 1998b].

Acknowledgments. This work was partially supported by the Office of Naval Research under grant N00014-94-1-0100 at Stanford University. S. A. Cummer was supported by a National Research Council Postdoctoral Research Associateship for a portion of this work. We thank A. Fraser-Smith of Stanford University for the use of the ELF-VLF radiometer and F. Perry Snyder of NCCOSC/NRaD

for helpful discussions regarding the LWPC propagation model.

References

Barr, R., The effect of sporadic-*E* on the nocturnal propagation of ELF waves, *J. Atmos. Terr. Phys., 39*, 1379-1387, 1977.

Bracewell, R. N., *The Fourier Transform and Its Applications*, McGraw-Hill, New York, 1986.

Bracewell, R. N., *Two-Dimensional Imaging*, Prentice-Hall, Englewood Cliffs, 1995.

Budden, K. G., *The Wave-Guide Mode Theory of Wave Propagation*, Logos Press, London, 1961.

Burke, C. P., and D. L. Jones, An experimental investigation of ELF attenuation rates in the Earth-ionosphere duct, *J. Atmos. Terr. Phys., 54*, 243-250, 1992.

Burke, C. P., and D. L. Jones, On the polarity and continuing currents in unusually large lightning flashes deduced from ELF events, *J. Atmos. Terr. Phys., 58*, 531-540, 1996.

Cooray, V., and C. Gomes, Estimation of peak return stroke currents, current time derivatives and return stroke velocities from measured fields, *J. Electrost., 43*, 163-172, 1998.

Cummer, S. A., U. S. Inan, and T. F. Bell, Ionospheric D region remote sensing using VLF radio atmospherics, *Radio Sci., 33*, 1781-1792, 1998a.

Cummer, S. A., U. S. Inan, T. F. Bell, and C. P. Barrington-Leigh, ELF radiation produced by electrical currents in sprites, *Geophys. Res. Lett., 25*, 1281-1284, 1998b.

Cummins, K. L., E. P. Krider, and M. D. Malone, The US National Lightning Detection Network (TM) and applications of cloud-to-ground lightning data by electric power, *IEEE Trans. Electromagn. Compat., 40*, 465-480, 1998.

Fraser-Smith, A. C., and R. A. Helliwell, The Stanford University ELF/VLF radiometer project: Measurement of the global distribution of ELF-VLF electromagnetic noise, *Proc. 1985 IEEE Internat. Symp. Electromagn. Compat.*, 305, 1985.

Greifinger, C., and P. Greifinger, Approximate method for determining ELF eigenvalues in the earth-ionosphere waveguide, *Radio Sci., 13*, 831-837, 1978.

Greifinger, C., and P. Greifinger, On the ionospheric parameters which govern high-latitude ELF propagation in the earth-ionosphere waveguide, *Radio Sci., 14*, 889-895, 1979.

Greifinger, C., and P. Greifinger, Noniterative procedure for calculating ELF mode constants in the anisotropic earth-ionosphere waveguide, *Radio Sci., 21*, 981-990, 1986.

Hepburn, F., Atmospheric waveforms with very low-frequency components below 1 kc/s known as slow tails, *J. Atmos. Terr. Phys., 10*, 266-287, 1957.

Hubert, P., P. Laroche, A. Eybert-Berard, and L. Barret, Triggered lightning in New Mexico, *J. Geophys. Res., 89*, 2511-2521, 1984.

Hughes, H. G., Differences between pulse trains of ELF atmospherics at widely separated locations, *J. Geophys. Res., 76*, 2116-2125, 1971.

Jones, D. L., Propagation of ELF pulses in the earth-ionosphere cavity and application to 'slow tail' atmospherics, *Radio Sci., 5*, 1153-1162, 1970.

Krehbiel, P. R., M. Brook, and R. A. McCrory, An analysis of the charge structure of lightning discharges to ground, *J. Geophys. Res., 84*, 2432-2456, 1979.

Lyons, W. A., Sprite observations above the U.S. High Plains in relation to their parent thunderstorm systems, *J. Geophys. Res., 101*, 29,641-29652, 1996.

Nickolaenko, A. P., Modern aspects of Schumann resonance studies, *J. Atmos. Sol. Terr. Phys., 59*, 805-816, 1997.

Pappert, R. A., and J. A. Ferguson, VLF/LF mode conversion model calculations for air to air transmissions in the Earth-ionosphere waveguide, *Radio Sci., 21*, 551-558, 1986.

Pappert, R. A., and W. F. Moler, Propagation theory and calculations at lower extremely low frequencies (ELF), *IEEE Trans. Commun., 22*, 438-451, 1974.

Press, W. H., S. A. Teukolsky, W. T. Vetterling, and B. P. Flannery, *Numerical Recipes in FORTRAN, 2nd ed.*, Cambridge Univ. Press, New York, 1992.

Rawer, K., D. Bilitza, and S. Ramakrishnan, Goals and status of the International Reference Ionosphere, *Rev. Geophys., 16*, 177-181, 1978.

Reising, S. C., U. S. Inan, T. F. Bell, and W. A. Lyons, Evidence for continuing current in sprite-producing cloud-to-ground lightning, *Geophys. Res. Lett., 23*, 3639-3642, 1996.

Segalovitz, A., and B. R. Frieden, A "CLEAN"-type deconvolution algorithm, *Astron. Astrophys., 70*, 335, 1978.

Sukhorukov, A. I., On the excitation of the Earth-ionosphere waveguide by pulsed ELF sources, *J. Atmos. Terr. Phys., 54*, 1337-1345, 1992.

Sukhorukov, A. I., ELF-VLF atmospheric waveforms

under night-time ionospheric conditions, *Ann. Geophys., 14*, 33-41, 1996.

Taranenko, Y. N., U. S. Inan, and T. F. Bell, Interaction with the lower ionosphere of electromagnetic pulses from lightning: Heating, attachment, and ionization, *Geophys. Res. Lett., 20*, 1539-1542, 1993.

Taylor, W. L., and K. Sao, ELF attenuation rates and phase velocities observed from slow-tail components of atmospherics, *Radio Sci., 5*, 1453-1460, 1970.

Thottappillil, R., V. A. Rakov, and M. A. Uman, Distribution of charge along the lightning channel: Relation to remote electric and magnetic fields and to return-stroke models, *J. Geophys. Res., 102*, 6987-7006, 1997.

Wait, J. R., On the theory of the slow-tail portion of atmospheric waveforms, *J. Geophys. Res., 65*, 1939-1957, 1960.

Weidman, C. D., and E. P. Krider, The amplitude spectra of lightning radiation fields in the interval from 1 to 20 MHz, *Radio Sci., 21*, 964-970, 1986.

S. A. Cummer, Department of Electrical and Computer Engineering, Duke University, Durham, NC 27708. (cummer@ee.duke.edu)

U. S. Inan, STAR Laboratory, Stanford University, Packard Bldg. Rm. 355, 350 Serra Mall, Stanford, CA 94305-9515.

(Received March 17, 1999; revised November 1, 1999; accepted November 2, 1999.)